*Proc. R. Soc. Lond.* A. **331**, 19–38 (1972)
*Printed in Great Britain*

# The measurement of van der Waals dispersion forces in the range 1.5 to 130 nm

BY J. N. ISRAELACHVILI AND D. TABOR, F.R.S.
*Surface Physics, Cavendish Laboratory, University of Cambridge, Free School Lane, Cambridge*

(*Received* 4 *April* 1972)

[Plate 1]

This paper describes an experimental study of the van der Waals dispersion forces between curved mica surfaces. For separations in the range 1.4 to 20 nm the forces were determined by the jump method described in earlier work by Tabor & Winterton (1969). For larger separations the forces were determined by a new dynamic method. One surface was supported on a rigid piezo-electric crystal and could be set vibrating at very small amplitudes over a convenient range of frequencies. The other was supported, facing it, on a stiff spring: its natural frequency depended both on the spring stiffness and on the van der Waals force exerted upon its by the first surface. By determining the resonant frequency as a function of separation the law of force was deduced in the range 10 to 130 nm. Both methods thus covered the range from 1.4 to 130 nm. In this way it is shown that there is a gradual transition between non-retarded and retarded forces as the separation is increased from 12 to 50 nm.

Experiments have also been carried out on the influence of adsorbed fatty acid monolayers on the van der Waals interaction between mica surfaces. The results show that for separations greater than about 5 nm the forces are as for bulk mica: for separations less than 3 nm the forces are slightly less and appear to be dominated by the van der Waals properties of the monolayers themselves.

## 1. INTRODUCTION

### *The nature of van der Waals forces*

The van der Waals forces between any two atoms or molecules may be separated into *orientation*, *induction* and *dispersion* forces. Orientation forces arise only in the case of polar molecules, that is molecules having permanent multipole moments, and may be explained in terms of the interaction between static dipoles, quadrupoles, etc. A polar molecule may also induce polarity in a nearby neutral molecule and this results in an attractive induction force between them.

With non-polar molecules none of the interactions which are caused by permanent dipoles can arise. However, the non-polarity of such molecules is a time average: if they are studied at very short intervals they are found to possess finite fluctuating dipole and higher multipole moments. These instantaneous moments induce polarity in neighbouring atoms or molecules to give an attractive force. The fluctuations involved have a frequency in the ultraviolet range and play an important part in optical dispersion: for this reason forces arising from this mechanism are known as dispersion van der Waals forces. For separations greater than about one nanometer the forces due to dipole–dipole dispersion interactions generally overshadow those due to dipole–quadrupole and higher multipole interactions, but for smaller separations multipole interactions assume increasing importance. Dispersion forces generally dominate over orientation and induction forces except in the case of strongly polar molecules. For example with water the orientation, induction and dispersive forces are in the ratio 20:1:3.5, while with hydrogen chloride the corresponding ratios are 2:0.5:10 on the same scale.

At small separations van der Waals forces may be large but they are usually weaker than chemical binding forces. On the other hand, for large separations they are weak compared with electrostatic forces. In the absence of chemical and electrostatic forces they are the sole attractive forces between atoms or molecules.† For example, the atoms in solid argon or the molecules in solid polyethylene are held together by van der Waals forces while the imperfect gas behaviour of real gases is due to them. The strength of van der Waals forces rises rapidly as atoms, molecules or bodies approach one another. They are usually attractive but in special circumstances they can be repulsive.

### *Theories of van der Waals dispersion forces*

Theories of dispersion forces are described as microscopic or macroscopic according to the method of approach. In microscopic theories the force between atoms and molecules is obtained in terms of their microscopic properties, for example the atomic or molecular polarizabilities. London (1930, 1937) published the first satisfactory microscopic theory of dipole–dipole dispersion forces for two neutral atoms by considering the perturbation in their zero-point energy. Treating them as isotropic harmonic oscillators of characteristic frequencies $\omega_1$ and $\omega_2$ and atomic polarizabilities $\alpha_1$ and $\alpha_2$ he showed that the potential energy when they are a distance $d$ apart is given by

$$U = -\frac{3\hbar}{2}\,\frac{\omega_1\omega_2}{\omega_1+\omega_2}\,\frac{\alpha_1\alpha_2}{d^6}. \tag{1}$$

If the atoms are an appreciable distance apart the time taken for the electrostatic field of one instantaneous dipole to reach a neighbouring atom and return may be comparable with the fluctuating period itself. In that case the dipole of the first atom is no longer in phase with its neighbour and the law of force changes. The interaction is now known as the retarded van der Waals interaction. Casimir & Polder (1948) by an extension of London's theory showed that for separations greater than $\lambda_i/2\pi$, where $\lambda_i$ are the characteristic absorption wavelengths, there is a progressively diminishing correlation between the polarizations of neighbouring atoms as $d$ increases, and the energy is given by

$$U = -\frac{23}{4\pi}\hbar c\,\frac{\alpha_{10}\alpha_{20}}{d^7}, \tag{2}$$

where $\alpha_{10}$, $\alpha_{20}$ are the static atomic polarizabilities. Thus as the distance $d$ increases above $\lambda_i/2\pi$ the non-retarded $1/d^6$ power law goes over to the retarded $1/d^7$ power law. The transition is gradual and may extend over several tens of nanometers.

† Certain spin interactions and relativistic effects between atoms (Power, Meath & Hirschfelder 1966) may, under certain circumstances, exceed any of the forces mentioned here. However, there is no evidence to suggest that these forces play any appreciable part in the forces between macroscopic bodies in the condensed state.

McLachlan (1963*a*, *b*, 1965) has presented a more general microscopic theory of dispersion forces – the 'Susceptibility' theory – which also takes into account the presence of a third medium between the interacting atoms.

From microscopic theories, such as those described above, the dispersion energy between two macroscopic bodies may be computed by straightforward pairwise energy summation assuming that van der Waals interaction energies, like gravitational potentials, are additive. In this way the force between bodies of various shapes may be found. For example, for two semi-infinite solids (two parallel flat plates) distance $D$ apart the force per unit area $f$ is

$$\text{for non-retarded forces: } f = A/6\pi D^3, \tag{3}$$

$$\text{and for retarded forces: } f = B/D^4, \tag{4}$$

where $A$ and $B$ are appropriate constants known as the Hamaker constants and are related to the constants in equations (1) and (2) respectively.

The assumption of simple additivity ignores the influence of neighbouring atoms on the interactions between any pair of atoms. Though these effects are small (Langbein 1969) the problem is very complicated. It is completely avoided in the macroscopic theory where the atomic structure is ignored and the forces between macroscopic bodies are derived in terms of such bulk properties as their dielectric constants.

The first general macroscopic theory is due to Dzyaloshinskii, Lifshitz & Pitaevskii (1961). They applied the methods of modern quantum field theory to obtain the dispersion force between two flat parallel plates 1 and 2 separated by distance $D$ by a third medium 3. *For non-retarded forces* the theory gives for the force per unit area $f$

$$f = \frac{\hbar}{8\pi^2 D^3}\int_0^\infty \sum_{n=1}^{\infty} \frac{1}{n^3}\left[\left(\frac{\epsilon_1-\epsilon_3}{\epsilon_1+\epsilon_3}\right)\left(\frac{\epsilon_2-\epsilon_3}{\epsilon_2+\epsilon_3}\right)\right]^n \mathrm{d}\xi$$

$$= \frac{\hbar}{8\pi D^3}\int_0^\infty \left(\frac{\epsilon_1-\epsilon_3}{\epsilon_1+\epsilon_3}\right)\left(\frac{\epsilon_2-\epsilon_3}{\epsilon_2+\epsilon_3}\right)\mathrm{d}\xi + \frac{\hbar}{8\pi^2 D^3}\int_0^\infty \frac{1}{8}\left(\frac{\epsilon_1-\epsilon_3}{\epsilon_1+\epsilon_3}\right)^2\left(\frac{\epsilon_2-\epsilon_3}{\epsilon_2+\epsilon_3}\right)^2 \mathrm{d}\xi + \dots \tag{5}$$

$$= \frac{A_{132}}{6\pi D^3}, \tag{6}$$

where $\epsilon_j = \epsilon_j(\mathrm{i}\xi)$ is the dielectric constant (or permittivity) of the $j$th medium as a function of an imaginary frequency i$\xi$, and $A$ is the Hamaker constant for non-retarded forces. In the case of most dielectrics the first term of equation (5) constitutes about 98 % of the total value of $f$.

For *retarded forces* the theory gives

$$f = \frac{\pi^2\hbar c}{240 D^4}\frac{1}{\epsilon_{30}^{\frac{1}{2}}}\left(\frac{\epsilon_{10}-\epsilon_{30}}{\epsilon_{10}+\epsilon_{30}}\right)\left(\frac{\epsilon_{20}-\epsilon_{30}}{\epsilon_{20}+\epsilon_{30}}\right)\Phi(\epsilon_{10}, \epsilon_{20}, \epsilon_{30}) \tag{7}$$

$$= B/D^4, \tag{8}$$

where $\epsilon_{10}$, $\epsilon_{20}$, $\epsilon_{30}$ are the static dielectric constants, and $\Phi(\epsilon_{10}, \epsilon_{20}, \epsilon_{30})$ is a function whose value lies between 1 and $69/2\pi^4$. $B$ is the Hamaker constant for retarded forces. The above two equations are applicable to all media (metals and dielectrics). Exact solutions are carried out by numerical methods once the dielectric data of the media are known over the whole spectral range. Krupp (1967) has calculated the dispersion forces for various solids 0.4 nm apart and has obtained values of $f$ in the range $(2\text{–}30) \times 10^7\,\mathrm{N/m^2}$. This of the order of the tensile strengths of solids.

The effects of adsorbed surface layers on the dispersion forces between macroscopic bodies have recently been studied theoretically by Langbein (1969, 1971, 1972) and Ninham & Parsegian (1970).

### *Van der Waals dispersion forces and electrostatic images*

Van der Waals dispersion forces are quantum mechanical in nature and the theories are rather complicated and mathematically lengthy. This tends to obscure the physical processes that give rise to them. In a succeeding paper an attempt has been made at a simple treatment of dispersion forces based on the method of images in electrostatics. Though no claim is made to mathematical rigour many of the important results that have been derived by means of more sophisticated methods, as well as some new results, are obtained in a way that is more easily understandable. For example, the method provides a conceptual explanation of repulsive forces. In addition an equation (see equation (22) below) is derived for the non-retarded forces between two bodies separated by a third medium in terms of an adsorption frequency and refractive index: no integration such as occurs in equation (5) is required.

### *Previous measurements of van der Waals forces*

As van der Waals forces are involved whenever bodies come into close proximity these forces play an important role in such diverse processes as colloidal stability, surface tension, the strengths of solids, adhesion, the behaviour of gases, the thinning of liquid films, the stability of lipid membranes, etc. Many of these systems have already been studied. However, experiments of this type to determine van der Waals forces are indirect, involving many parameters which themselves are uncertain.

The most satisfactory study of van der Waals forces involves simpler, more direct experimental procedures. The method commonly used is to position two bodies close together and to measure the force of attraction as a function of the distance between them. Most of the measurements carried out in the fifties and sixties were of this type: the bodies were made of glass, the force was determined by measuring the deflexion of a balance arm, and the distance between the highly polished surfaces obtained by optical interference. In this way the van der Waals forces between various types of glass were successfully measured in the range 25 to 1200 nm and confirmed the existence of retarded forces.

In all these experiments three problems were invariably encountered:

(1) Vibrations from the surrounding always found their way into the sensitive

moving parts of the apparatus and could never be completely suppressed. The effect of vibrations was to prevent accurate measurements from being made at large separations where the forces are very weak. Hence the upper limit of 1200 nm.

(2) Protruding surface asperities of the order of 5 to 20 nm, small dust particles, and a layer of silica gel, were always found to be present on the glass surfaces and these prevented measurements from being made at separations smaller than several tens of nanometers. It is only in the last year (Rouweler & Overbeek 1971) that the first successful measurements below 80 nm were made on glass surfaces – a consequence of improvements in surface preparation.

(3) Electrostatic charges on the surfaces often gave rise to spurious results. Several techniques were applied by which these could be detected and removed.

The first measurements of this type were by Derjaguin and his school in Russia (see, for example, Derjaguin, Abrikossova & Lifshitz 1956), by Sparnaay (1952, in 1958) Holland and by Kitchener & Prosser (1957) in Britain. The best results to date on glass are undoubtedly those of the Dutch school (Black, de Jongh, Overbeek & Sparnaay (1960); Sparnaay & Jochems (1960); Van Silfhout (1966); Rouweler & Overbeek (1971)). Rouweler & Oberbeek (1971) measured the dispersion force between a fused silica glass lens and a flat in the range 25 to 350 nm. Above 50 nm retarded forces were observed, while at shorter distances a transition towards non-retarded forces was detected.

A new experimental method due to Hunklinger (1969) avoided the problem of vibrations. One of the surfaces was made to vibrate at a known amplitude, and the amplitude of vibrations induced in the other was measured. In this way the van der Waals law of force was obtained in the range 80 to 1200 nm.

In general, agreement between experiment and theory is good: the correct power law for retarded forces is obtained, and the values found for the magnitude of the forces agree within a factor of two. It is, however, worth noting that the so-called 'theoretical' values are themselves calculated in terms of often scanty experimental data.

In 1969 Tabor & Winterton measured the van der Waals forces between two mica surfaces. Mica is one of the few materials with a surface that is molecularly smooth over fairly large areas, and for this reason it was possible to measure the forces from 30 nm down to 5 nm – the first successful measurement in the non-retarded region. As the work to be described is essentially an extension of the Tabor & Winterton work we shall leave further reference to it until later.

## 2. Experimental method and procedure

An apparatus was constructed to measure the van der Waals forces between two crossed cylindrical sheets of muscovite mica. The contact resembles that between a sphere and a flat. Two mica sheets, a few micrometres thick, were first silvered on one side and then glued to two glass sections that had been cut out from cylindrical tubes. The sheets were glued with their unsilvered surfaces exposed. The glass sections were then mounted into the apparatus so as to face each other with their axes at right angles (figure 1). The distance between the surfaces was measured to about $\pm 0.2$ nm by allowing white light to pass through them and observing the interference fringes (fringes of equal chromatic order or f.e.c.o.) spectrometrically. For details of the optical method see Tabor & Winterton (1969).

The van der Waals forces were measured by two different methods: (1) by the 'jump method', in the range 1.5 to 20 nm, and (2) by the 'resonance method', in the range 10 to 130 nm.

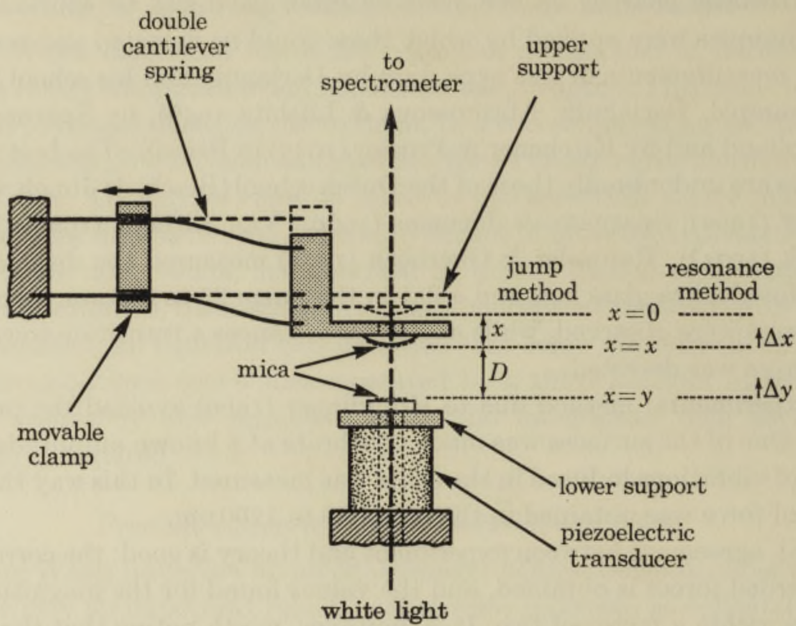


FIGURE 1 (*a*). Schematic drawing on the main parts of the apparatus. In jump experiments a double cantilever spring was used. In resonance experiments a single cantilever 'bimorph' spring was used as shown in figure 1 (*b*), plate 1.

## *Method* 1. *The jump method*

The lower glass section (figure 1) is attached to a rigid base capable of vertical displacement through a total distance of about 2 mm, with control better than 0.1 nm. The larger movement was achieved with a two-lever system operated by a motor-driven micrometer screw while the fine control was obtained with a piezoelectric transducer of sensitivity 0.4 nm/V for finally bringing the surfaces towards each other.

The upper glass section is mounted at the end of a double or single cantilever spring. If the lower surface is moved towards the upper, at some point – depending on the stiffness of the spring – the two will jump into contact. The measurement of this jump distance as a function of the spring stiffness is the basis of the jump method. The theory is as follows.

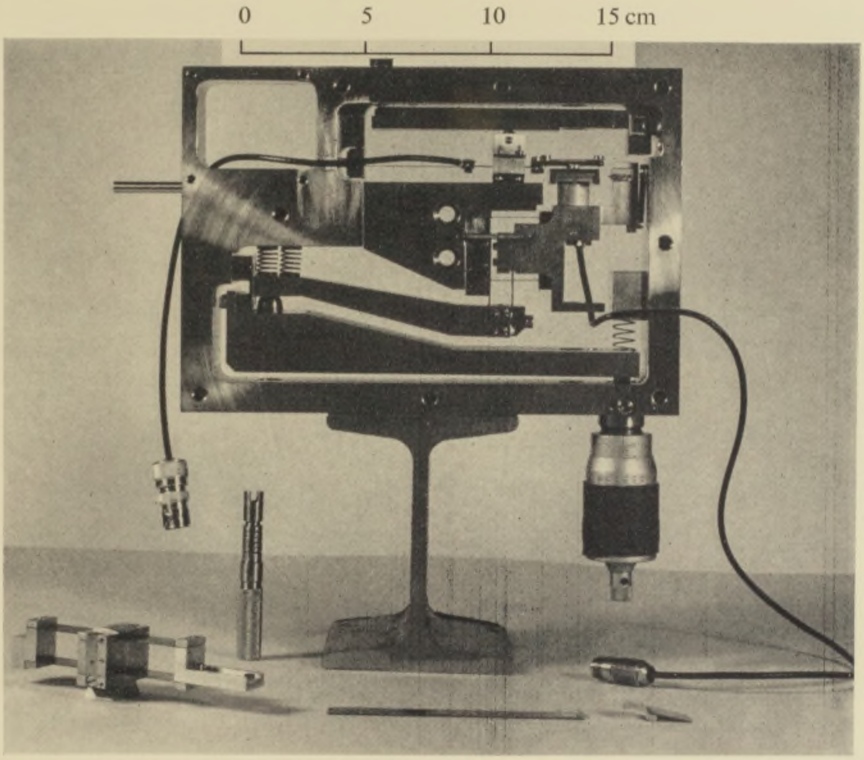


FIGURE 1 (*b*). Photograph of apparatus as used in resonance experiments. The parts for use in jump experiments are on the bottom left.

(*Facing p.* 24)

When the surfaces are a large distance $D$ apart there is no van der Waals interaction between them and the equilibrium position of the upper surface is at $x = 0$. As the lower support is moved upwards the increasing van der Waals attraction pulls the upper support down to a new equilibrium position where the spring deflexion $= x$: here the van der Waals attractive force $\mathscr{C}/D^n$ is balanced by the restoring force of the spring $Kx$, so that at equilibrium we have

$$F = \mathscr{C}/D^n - Kx = 0. \tag{9}$$

The jump occurs when the gradients of the van der Waals and spring forces are balanced, i.e. when

$$\mathrm{d}F = -\frac{n\mathscr{C}}{D^{n+1}}\mathrm{d}D - K\,\mathrm{d}x = 0. \tag{10}$$

But $\mathrm{d}x = -\mathrm{d}D$. This gives the jump distance $D_0$ as

$$D_0 = \left(\frac{n\mathscr{C}}{K}\right)^{1/(n+1)}. \tag{11}$$

Thus a graph of $\lg K$ against $\lg D_0$ should give a straight line of slope $-1/(n+1)$ from which the constant $\mathscr{C}$ may also be determined. For crossed cylinders of radius $R$ theory predicts that

$$\text{for non-retarded forces: } F = AR/6D^2 \quad \text{i.e.} \quad \mathscr{C} = \tfrac{1}{6}AR, \quad n = 2, \tag{12}$$

$$\text{for retarded forces: } F = 2\pi BR/3D^3 \quad \text{i.e.} \quad \mathscr{C} = \tfrac{2}{3}\pi BR, \quad n = 3, \tag{13}$$

where $A$ and $B$ are the Hamaker constants for non-retarded and retarded van der Waals forces.

Thus to find $A$ and $B$ by the jump method we require to measure $D_0$, $R$ and $K$. The jump distance $D_0$ was measured to 4% from the shift in wavelength of the f.e.c.o. fringes at the jump; the radius $R$ was measured to about 10% from the shape of the fringes, and the stiffness $K$ determined by measuring the natural frequency $f_\infty$ of vibration of the upper support: this is related to $K$ by the equation $f_\infty = (K/m)^{\frac{1}{2}}/2\pi$ where $m$ is the inertia of the support. A known mass was attached to the upper support and from the new natural frequency the inertia term was eliminated and $K$ calculated.

There is also a contribution to the stiffness from the inherent stiffness of the lever system, the mountings and the glue layer supporting the mica sheets. This remains fixed throughout an experiment and was determined by squeezing the surfaces together with a known force and measuring, with a sensitive dial gauge, the approach of the supports. In this way the overall stiffness could be measured at each clamping position to an accuracy of about 3%.

The jump method was previously used by Tabor & Winterton (1969) to measure forces between mica surfaces in the range 5 to 30 nm. In their apparatus the spring stiffness was varied by fitting a new spring to the upper support. This meant that a complete experiment had to be carried out for each new point on the graph of $\lg K$ against $\lg D_0$: new mica sheets had often to be prepared and mounted into the apparatus; the optics realined; the radius of the surfaces measured, and the spring stiffness recalibrated. As a result much time and consistency were lost.

In the new apparatus these defects were overcome by using a cantilever spring whose stiffness $K$ could be varied by adjusting the clamping position along its length: and as the stiffness of a cantilever spring is proportional to the inverse cube of its free length a very wide range of stiffness was thereby achieved. With this arrangement the jump method proved effective for separations ranging from 2 to 20 nm in the case of clean mica surfaces, and in the range 1.4 to 20 nm for mica surfaces each coated with a monolayer of stearic acid. Accurate measurements of larger jumps proved impossible owing to vibrations – larger jumps requiring weaker spings, which are more sensitive to external disturbances. The smallest jump distance could not be reduced below 1.4 nm: this was determined by the maximum stiffness attainable with the apparatus.

### *Method 2. The resonance method*

As vibrations made it impossible to use the jump method for accurate measurements much above 20 nm some other method had to be devised suitable for the larger distances. This is the resonance method.

Consider the two mica surfaces of figure 1 a large distance $D$ apart so that there is a negligible van der Waals interaction between them. The natural frequency of mechanical vibrations of the upper support $f_\infty$ will depend on the spring stiffness and on the inertia of the support. If the two surfaces are now made to approach each other the increasing van der Waals attraction between them will cause the natural frequency to fall below $f_\infty$ until, at the jump separation, the natural frequency is zero.

The principle of the resonance method is to measure the resonant frequency $f_D$ of the upper support as a function of the gap distance $D$, and from this to deduce the law of force in the range of distances measured.

In a resonance experiment the spring of the upper support is fairly stiff and remains fixed throughout the experiment. The spring is made of piezoelectric material and serves both for a spring and a strain gauge. (In our experiments a piezoelectric 'bimorph' strip was used, made by Vernitron Ltd, Southampton.) Thus vibrations of the upper support were measured from the output voltage generated by the vibrating spring whose sensitivity was of the order of 1 mV/nm, but also included noise.

One of the main differences between the jump and resonance methods concerns air damping. The jump method is carried out at atmospheric pressure; here the air in the gap between the surfaces is an advantage since it damps out the vibrations of the upper surface. If the resonance experiments were to be carried out in air at atmospheric pressure the damping would be above critical. It is desirable to reduce air damping to negligible proportions. This was achieved by mounting the apparatus in a large chamber which could be evacuated to about $5 \times 10^{-5}$ mmHg ($\approx$ 7 mPa).

A brief account of the theory of the resonance method is as follows. Let the lower support vibrate with angular frequency $p$ ($p = 2\pi f$) and small amplitude $\Delta y$ (figure 1). This will induce vibrations in the upper support of angular frequency $p$ and amplitude $\Delta x$. We can therefore write:

for the upper support: $x = x + \Delta x\,\mathrm{e}^{\mathrm{i}pt}$,

for the lower support: $y = y + \Delta y\,\mathrm{e}^{\mathrm{i}(pt+\theta)}$,

for the separation: $D = y - x = D + (\Delta y\,\mathrm{e}^{\mathrm{i}\theta} - \Delta x)\,\mathrm{e}^{\mathrm{i}pt} = D + \Delta D\,\mathrm{e}^{\mathrm{i}pt}$,

which can be substituted into equation (9) to give the equation of motion of the upper support:

$$\Delta F = \frac{\mathscr{C}}{(D + \Delta D\,\mathrm{e}^{\mathrm{i}pt})^n} - K(x + \Delta x\,\mathrm{e}^{\mathrm{i}pt}) = m\ddot{x}, \tag{14}$$

where $m$ is the inertia of the upper support.

Although the damping due to air is negligible there remains another contribution to the damping from the internal friction of the piezoelectric bimorph strip. This may be taken into account by introducing a viscous damping term $\gamma\dot{x}$ into equation (14). The resulting expression may be simplified and put in more convenient form in terms of the natural frequency at infinite separation $p_\infty$ and the jump distance $D_0$, defined by

$$p_\infty = (K/m)^{\frac{1}{2}} = 2\pi f_\infty, \quad D_0 = (n\mathscr{C}/K)^{1/(n+1)},$$

from which we finally obtain the general equation of motion for forced oscillations of the damped system:

$$\left|\frac{\Delta x}{\Delta y}\right| \mathrm{e}^{-\mathrm{i}\theta} = \frac{(D_0/D)^{n+1} p_\infty^2}{\{(p^2 - p_D^2) + \mathrm{i}\gamma p/m\}}. \tag{15}$$

The term $p_D$ in the denominator of equation (15) is the resonant angular frequency of the upper support when the surfaces are distance $D$ apart. This may be expressed in terms of the natural angular frequency $p_\infty$ when $D = \infty$ by the relation

$$p_D = p_\infty[1 - (D_0/D)^{n+1}]^{\frac{1}{2}}. \tag{16}$$

This expression shows that when $D = D_0$ the upper support has zero frequency since it is in a force field which locally shows no variation with displacement ($\partial F/\partial x = 0$). As $D$ increases above $D_0$ the resonant frequency rises, at first sharply and then more gradually, converging towards $p_\infty$ as $D$ approaches infinity. This is the equation which forms the basis of the resonance method.

From equation (15) we also obtain the phase difference $\theta$ between the two vibrating surfaces:

$$\theta = \tan^{-1}\left[\frac{\gamma p}{m(p^2 - p_D^2)}\right] = \arctan\left[\frac{\gamma f}{2\pi m(f^2 - f_D^2)}\right]. \tag{17}$$

It is also sometimes convenient to express the damping in terms of a quality factor $Q$ defined by

$$Q = p_D m/\gamma.$$

In most resonance experiments $Q \approx 50$.

Equation (17) shows that when the vibrations $\Delta y$ and $\Delta x$ of the surfaces are exactly out of phase ($\theta = 90°$) then $f = f_D$. This provided the method of determining the resonant frequency $f_D$. An a.c. voltage from a high-stability oscillator was applied across the piezoelectric transducer making the lower surface vibrate at a very small amplitude of about 0.1 nm and at a frequency $f$ slightly below $f_D$. This induced vibrations in the upper surface by the coupling provided by the van der Waals interaction. The input signal of the piezoelectric transducer and the output signal of the piezoelectric bimorph strip were both fed into a lock-in amplifier system (Brookdeal Electronics Ltd, type 40) which measured the relative phases of the vibrating supports, and was set so as to give a zero meter reading when $\theta = 90°$. The separation $D$ was slowly varied while the forcing frequency $f$ was kept fixed, and the value of $D$ at which the pointer on the meter passed through the zero position recorded: this is the value of $D$ for which $f = f_D$.

The values of $D$ and $f$ ($= f_D$) were recorded and the measurements repeated at different values of $f$. It was possible to make about 10 readings of $D$ and $f_D$, covering the range 10 to 130 nm, in $\frac{1}{2}$ h. Typical values of $D_0$ and $f_\infty$ were $D_0 \approx 8$ nm, $f_\infty \approx 100$ Hz.

The major advantage of using the phase difference as a means of determining the resonant frequency is that when $f = f_D$ the value of $\theta$ is 90° whatever the value of the damping constant $\gamma$ (provided it is not so large as to give critical damping). Indeed the damping only determines the sharpness of the sweep through the null reading around $\theta = 90°$, it does not introduce any error in the final result.

The accuracy of the method is high for the following reasons:

(1) As the forcing frequency $f = f_D$ is stable and measurable to at least 1 part in $10^6$ it is possible to make accurate measurements at large separations where $f_D$ and $f_\infty$ differ by no more than 1 part in $10^5$.

(2) The position of the fringes is recorded at a null reading of the meter, so that – as with all null methods – there is no systematic error in the values of $D$ so measured. The values of $D$ could be measured as accurately as the optics allowed, i.e. to about $\pm 0.2$ nm.

(3) It is not necessary to have large amplitudes of vibrations in order to make accurate measurements. The electronic measuring instruments were sufficiently sensitive for readings to be made when amplitudes no greater than 0.1 nm were used. It may also be shown that at these small amplitudes the effects of nonlinearity in the oscillations may be ignored.

(4) The problem of extraneous vibrations does not arise. Random vibrations in the upper support appear as noise in the output signal of the bimorph strip; this noise is effectively eliminated in the lock-in amplifier system which only selects that component in the signal that is of the same frequency as the forcing frequency.

One serious source of error resulted from the high sensitivity of the piezoelectric bimorph strip to temperature variations. Throughout the course of an experimental run in which frequencies are being measured to 1 part in $10^6$, it is essential that the natural frequency $f_\infty$ of the upper support also remains constant to 1 part in $10^6$. This is especially important when measurements are being made at larger separations where a change in $f_D$ of only 1 part in $10^4$ changes the resonance position $D$ by as much as 60 nm. Unfortunately, even the slightest variations in temperature gave rise to noticeable changes in the viscoelasticity of the bimorph, manifested by corresponding variations in $f_\infty$ by as much as 1 part in $10^5$ during the course of an experimental run.

In practice, the apparatus was evacuated and the temperature allowed to stabilize for about 10 h before the first measurements were taken, but long-term drifts were never quite successfully eliminated. Thus during some experiments the value of $f_\infty$ would progressively rise, while in others it would fall. Bearing this in mind it was possible to fix the limits of error in the measurements of $D$.

## 3. Results

The van der Waals forces were measured in the range 1.5 to 20 nm by the jump method, and in the range 10 to 130 nm by the resonance method. In the region

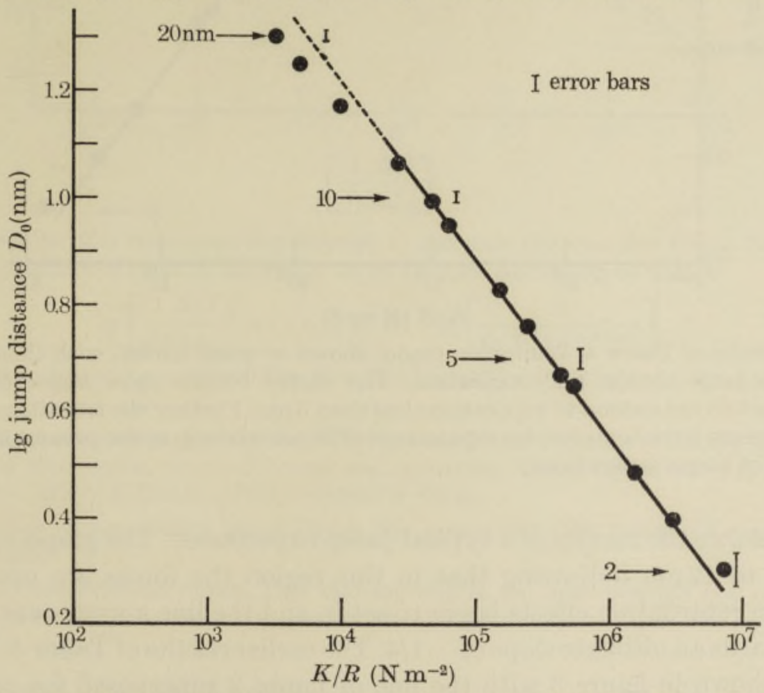


FIGURE 2. Results of jump experiments to measure the van der Waals force between crossed cylinders of mica in the range 2 to 20 nm. In the non-retarded region of force equations (11) and (12) predict the following relation between $D_0$ and $(K/R)$:

$$D_0 = \left\{\frac{nA}{6(K/R)}\right\}^{1/(n+1)},$$

where $D_0$ is the jump distance (nm), $K$ the stiffness (N/m), $R$ the radius of surfaces (m), $A$ the Hamaker non-retarded force constant (J) and $n$ the power law of the law of force. The results show that below 12 nm the forces are non-retarded with $n = 2.0 \pm 0.1$, $A = (1.35 \pm 0.15)\,10^{-19}$ J. Above 12 nm retardation effects begin to set in and by 20 nm the power law has increased to $n \approx 2.4$.

where the measurements of the two methods overlapped (i.e. between 10 and 20 nm) the results, both as regards the magnitude of the force and the power law, were in complete agreement.

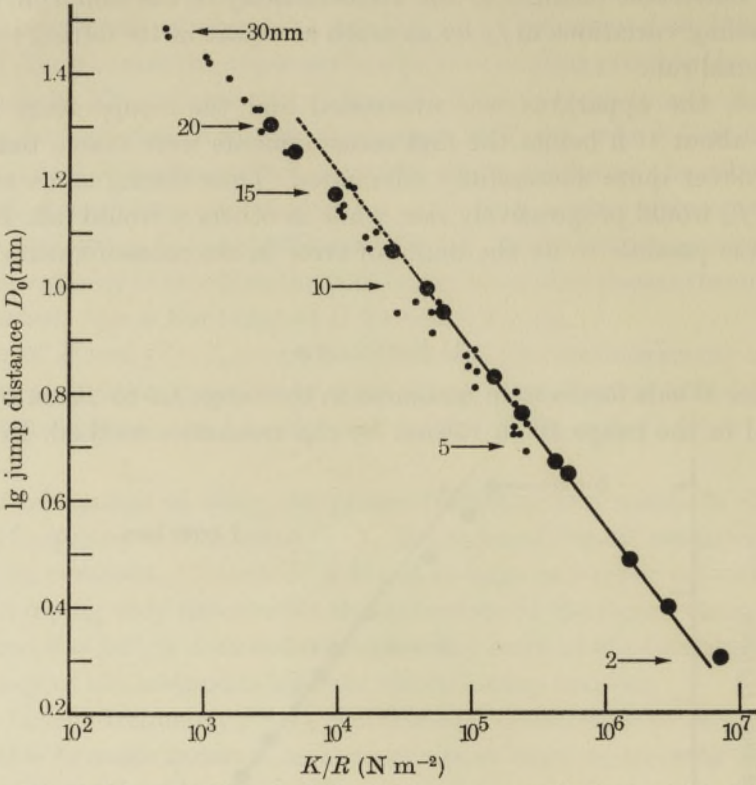


FIGURE 3. Results of Tabor & Winterton (1969) shown as small circles, with those of figure 2 shown as large circles, for comparison. The earlier results show larger experimental scatter and do not extend to separations less than 5 nm. Further the transition to retarded forces appears to be complete for separations of 30 nm whereas in the present investigation it occurs at larger separations.

Figure 2 shows the results of a typical jump experiment. The graph is a straight line from 2 to 12 nm indicating that in this region the forces are non-retarded. Above 12 nm retardation effects begin to set in and the line curves over gradually, tending towards an ultimate slope of $-1/4$. The earlier results of Tabor & Winterton (1969) are shown in figure 3 with the line of figure 2 superposed for comparison. The agreement is good, though the scatter of points in their graph is much greater – a result of the larger error in the radius of the surfaces, which had to be measured separately for each point. Tabor & Winterton's measurements extended to 30 nm, and between 20 and 30 nm their line gives $n \approx 3$ so that it was concluded that above 20 nm the forces are already completely retarded. However, they were not aware that as the amplitude of vibrations progressively increases the measured jump progressively decreases below the true value. Thus in all probability their line above 20 nm slopes towards a retarded power law too early.

The results of resonance experiments may also be presented graphically by plotting natural frequency $f_D$ against distance $D$; the curve may then be analysed by fitting it to equation (16). However, for a qualitative as well as a quantitative understanding of the results a straight line graph is more desirable.

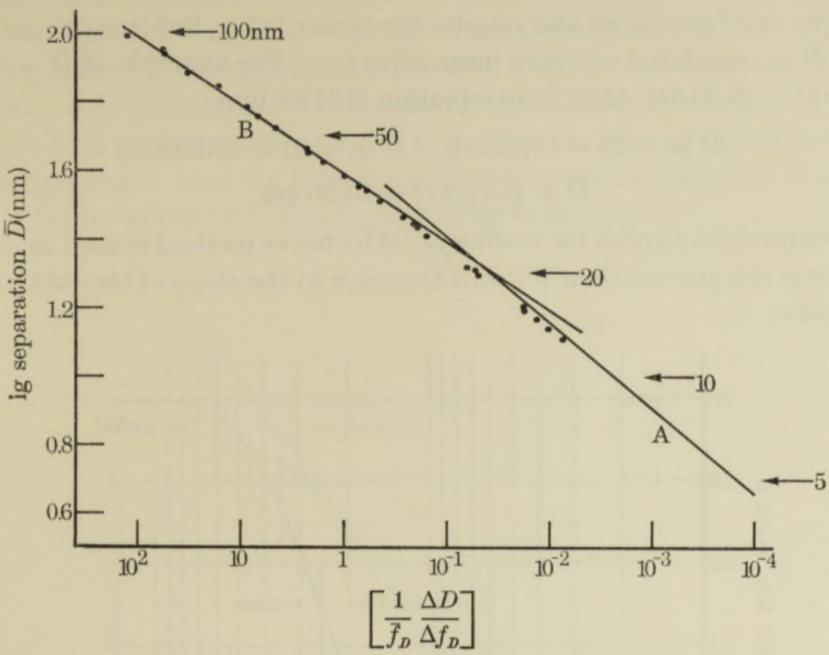


FIGURE 4. Results of a resonance experiment to measure the van der Waals force between crossed cylinders of mica in the range 10 to 130 nm. According to theory

$$\lg\left[\frac{1}{\bar{f}_D}\frac{\Delta D}{\Delta f_D}\right] = (n+2)\lg(\bar{D}) + \lg\left[\frac{2}{(n+1)\,D_0^{n+1} f_\infty^2}\right].$$

In this experiment $f_\infty = 109.00$ Hz, $K = (2.57 \pm 0.03) \times 10^3$ N/m, and $R = (1.58 \times 0.05) \times 10^{-2}$ m.

*Line B: retarded forces.* From points above about 50 nm we find $n = 3.0$, $D_0 = 7.8 \pm 0.1$ nm so that in this region retarded forces are operating. Using equations (11) and (13) we obtain $B = 3D_0^{n+1}K/2\pi nR = (0.97 \pm 0.06)\,10^{-28}$ J m.

*Transition region.* Below about 50 nm the power law falls below 3.0 reaching 2.2 at about 17 nm.

*Line A: non-retarded forces.* This line represents the non-retarded law of force with $n = 2$ as determined by the jump method for distances below 12 nm.

Differentiation of equation (16) gives

$$\lg\left[\frac{1}{f_D}\frac{\mathrm{d}D}{\mathrm{d}f_D}\right] = (n+2)\lg(D) + \lg\left[\frac{2}{(n+1)\,D_0^{n+1} f_\infty^2}\right]. \tag{18}$$

Consider two readings at $D$ and $D + \Delta D$ where the measured frequencies are $f_D$ and $f_D + \Delta f_D$. A graph of $\lg(\mathrm{d}D/f_D\,\mathrm{d}f_D)$ plotted against $\lg D$ should therefore give a line of slope $(n+2)$ from which the value of $D_0$ may also be determined. The van der Waals force constants $A$ and $B$ may then be determined from equations (11) to (13).

It may be shown that the value of $D$, say $\bar{D}$, against which $\Delta D/f_D \Delta f_D$ is to be plotted is not the mean of $D$ and $D+\Delta D$, but is given by

$$\bar{D} = D\left[\frac{(n+1)(\Delta D/D)}{\{1-(1+\Delta D/D)^{-(n+1)}\}}\right]^{1/(n+2)} = D + \frac{\Delta D}{2} - \frac{n+3}{24}\frac{\Delta D^2}{D} + \dots. \tag{19}$$

To find $\bar{D}$ by this formula we also require the power law $n$, but it turns out that the values of $\bar{D}$ so calculated are very insensitive to $n$. For example, if $D = 14.36$ nm, and $D+\Delta D = 18.03$ nm, then from equation (19) we find

$$\bar{D}\ (n=2) = 16.02\,\text{nm}, \quad \bar{D}\ (n=3) = 15.99\,\text{nm};$$

cf.

$$\bar{D} = D + \tfrac{1}{2}\Delta D = 16.20\,\text{nm}.$$

A similar expression applies for finding $\bar{f}_D$. Whichever method is used to determine $\bar{D}$ the error is not greater than 2 % but the error in the slope of the curve is appreciably greater.

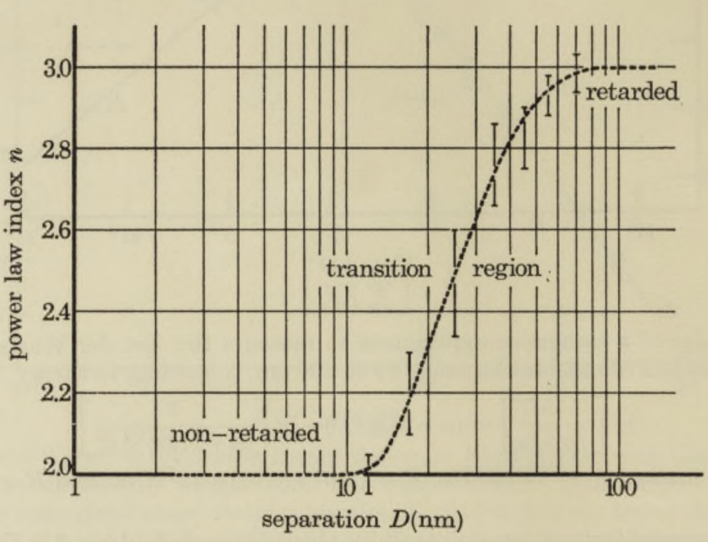


FIGURE 5. Variation of the power law $n$ of the van der Waals law of force between crossed mica cylinders with distance $D$. The curve is based on the combined results of a number of jump and resonance experiments.

The results of a number of resonance experiments carried out with one pair of mica specimens is shown in figure 4. Below 10 nm the 'equivalent' jump experiments results have also been added.

Figure 5 shows how the power law $n$ varies with distance.

The results of the jump and resonance experiments on the van der Waals law of force between crossed cylinders of mica may be summarized as follows:

*Non-retarded forces.* In the range 2 to 12 nm the force is completely non-retarded with

$$A = (1.35 \pm 0.15) \times 10^{-19}\,\text{J}, \quad n = 2.0 \pm 0.1.$$

*Transition region.* For separations greater than 12 nm the power law increases above 2.0 and by 50 nm has reached 2.9. Thus the transition between non-retarded and retarded forces may be said to occur between 12 nm and 50 nm.

*Retarded forces.* Above 50 nm the force is retarded with

$$B = (0.97 \pm 0.06) \times 10^{-28}\,\mathrm{J\,m}, \quad n = 3.0 \pm 0.1.$$

*Influence of monolayers on the surface forces.* Jump experiments were also carried out with a monomolecular layer of stearic acid on each mica surface deposited from a Langmuir–Blodgett trough in the conventional manner. The jump distance $D_0$ as determined from the fringes is the separation between the outermost $CH_3$ groups of the stearic acid monolayers. The results of one experiment are shown in figure 6 and suggest that for separations greater than 5 nm the force is the same as for bulk mica, but that below 3 nm the force remains non-retarded (with $n = 2$) though the value of $A$ is now about 75 % less than that for bulk mica.

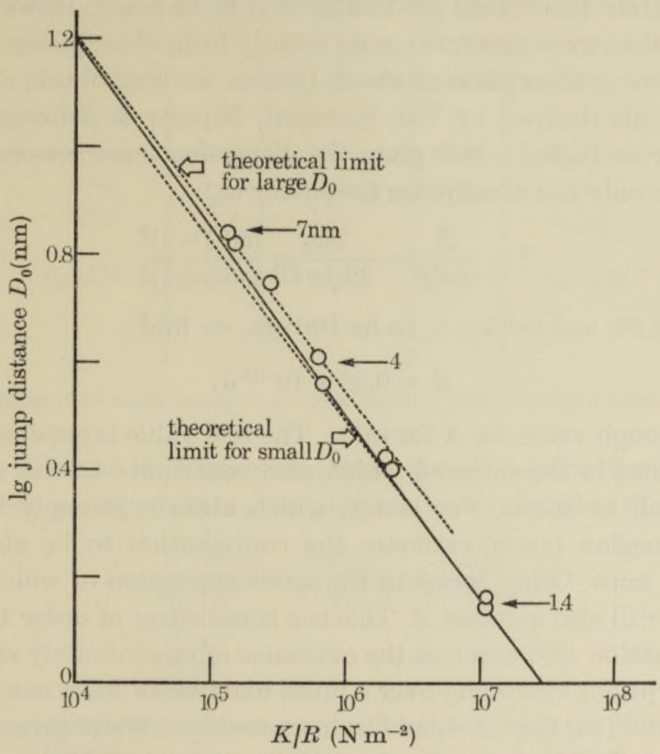


FIGURE 6. Results of a jump experiment to measure the van der Waals force in the range 1.4 to 7 nm between two mica surfaces with a monolayer of stearic acid on each. The continuous line is the theoretical curve based on equation (21). It is seen that above 5 nm the force is non-retarded and the force constant $A$ is as for bulk mica. Below 3 nm the force remains non-retarded but $A$ is now about 75 % of the mica value.

## 4. Comparison of results with theory and discussion

### *Retarded forces and the constant B*

Richmond & Ninham (to be published) collected all the current available data on the dielectric susceptibility of Muscovite mica, integrated the Lifshitz equation, and obtained a theoretical value for the constant $B$ of

$$B = 0.93 \times 10^{-28}\,\mathrm{J\,m}$$

which is in complete agreement with our experimental result of

$$B = (0.97 \pm 0.06) \times 10^{-28}\,\mathrm{J\,m}.$$

One may also obtain an approximate value for $B$ from equation (7). In the optical region the refractive index of mica is 1.60, thus putting $\epsilon_{10} = \epsilon_{20} = 1.60^2 = 2.56$, $\epsilon_{30} = 1$, $\Phi = 69/2\pi^4$ equation (7) gives

$$B = 0.88 \times 10^{-28}\,\mathrm{J\,m}.$$

*Non-retarded forces and the constant $A$*

Unfortunately, not enough detail is known of the dielectric properties of muscovite mica for an accurate theoretical prediction of $A$ to be made. However, as the non-retarded forces that were measured arise mainly from absorptions in the u.v., and as mica shows strong absorption at about 100 nm, we may obtain an estimate of $A$ by using a formula derived by Van Kampen, Nijboer & Schram (1968) and by Tabor & Winterton (1969) which gives the dispersion force between two identical media that have only one absorption frequency $\omega_0$:

$$f = \frac{A}{6\pi D^3} = \frac{\hbar\omega_0}{32\sqrt{\pi}\,D^3}\,\frac{(\epsilon(0)-1)^2}{(\epsilon(0)+1)^{\frac{3}{2}}}. \tag{20}$$

Putting $\epsilon(0) = 2.56$, and taking $\lambda_0$ to be 100 nm, we find

$$A = 0.95 \times 10^{-19}\,\mathrm{J}.$$

This gives a rough value for $A$ for mica. The real value is expected to be greater due to absorptions in the infrared which also contribute to the value of $A$, but these are difficult to assess. For water, which absorbs strongly in the infrared, Ninham & Parsegian (1970) estimate the contribution to be about 20 %. One expects less for mica. Other terms in the series expansion of which equation (20) is only the first will also increase $A$. This is a small effect of order 1 to 2 %. On the other hand, equation (20) assumes the existence of one infinitely sharp absorption peak. For absorptions extending over a finite bandwidth $\Delta\omega$ it can be shown using equations (23) and (24) that $A$ should be increased by a factor given approximately by $1 + \frac{3}{8}(\Delta\omega/\omega_0)^2$. In the case of mica $(\Delta\omega/\omega_0) \approx \frac{1}{2}$ (A. F. Vickers, private communication). This implies an increase of about 10 %. In view of these limitations the estimate obtained by means of equation (20) is in reasonable agreement with our experimental result of $(1.35 \pm 0.15) \times 10^{-19}\,\mathrm{J}$.

*Influence of adsorbed monolayers*

We first make a theoretical estimate of the Hamaker constant $A$ of stearic acid in monolayer form. By an interferometric technique described elsewhere (Israelachvili 1971) we were able to show that the stearic acid monolayers deposited on the mica had a thickness of $2.5 \pm 0.1$ nm and a refractive index of $1.50 \pm 0.01$. As the X-ray length of the stearic acid molecule is 2.44 nm we may conclude that the molecules are oriented with their chains normal to the mica surface. Consequently the refractive index found for the monolayers is for light travelling parallel to the hydrocarbon chains and agrees with the value 1.51 quoted for crystalline stearic acid (Winchell 1954). The two monolayers are absorbed with their carboxyl groups attached to the mica surfaces so that the polar groups of each layer are always more than 50 nm apart. It is therefore reasonable to assume that the dispersion forces between two monolayers are due essentially to the interaction between their hydrocarbon chains.

Adsorption spectra for long chain $n$-alkanes show a single sharp absorption peak at $\lambda_0 = 80$ nm (Schoen 1962; Koch & Skibowski 1971). It this also applies to the monolayers we may put $\epsilon(0) = 1.5^2 = 2.25$ and $\lambda_0 = 80$ nm into equation (20). We find for stearic acid

$$A = 0.88 \times 10^{-19}\,\mathrm{J}.$$

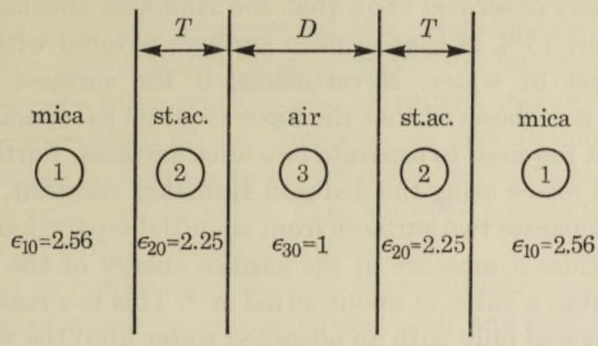


FIGURE 7. Arrangement of mica surfaces covered with adsorbed layers of stearic acid (st. ac.).

According to Ninham & Parsegian (1970) the dispersion force for the mica-monolayer system (see figure 7) is given approximately by the relation

$$\begin{aligned} f &= \frac{1}{6\pi}\left[\frac{A_{232}}{D^3} - \frac{2A_{123}}{(D+T)^3} + \frac{A_{121}}{(D+2T)^3}\right] \\ &= \frac{A_{\mathrm{eff}}}{6\pi D^3}, \end{aligned} \tag{21}$$

where $A_{ikj}$ represents the Hamaker constant for the interaction between two bodies $i$ and $j$ when separated by a third medium $k$, and is defined by equation (6). Thus the effective Hamaker constant $A_{\mathrm{eff}}$ should vary with separation $D$. At small separations ($D < T$) it should tend towards $A_{232}$ (that is monolayer–air–monolayer) and at large separations ($D > T$) towards $A_{232} - 2A_{123} + A_{121}$ which may be shown to be very nearly equal to $A_{131}$ (that is mica–air–mica). For simplicity we may assume all the media to have the same absorption frequency $\omega_0$. By a method similar to that used in deriving equation (20) we then obtain (see following paper)

$$A_{132} = \frac{3\hbar\omega_0}{8\sqrt{2}}\,\frac{(\epsilon_{10}-\epsilon_{30})\,(\epsilon_{20}-\epsilon_{30})}{(\epsilon_{10}+\epsilon_{30})^{\frac{1}{2}}\,(\epsilon_{20}+\epsilon_{30})^{\frac{1}{2}}\,[(\epsilon_{10}+\epsilon_{30})^{\frac{1}{2}}+(\epsilon_{20}+\epsilon_{30})^{\frac{1}{2}}]}, \tag{22}$$

which yields $A_{232} = 0.88 \times 10^{-19}$ J, $A_{123} = -0.16 \times 10^{-19}$ J and $A_{121} = 0.03 \times 10^{-19}$ J. By inserting these values and $T = 2.5$ nm into equation (21) we may calculate the way in which the jump distance should vary with separation. The calculated curve is shown in figure 6, together with the experimental results. It is seen that, in agreement with the predictions of Langbein (1969, 1971) and Ninham & Parsegian (1970), the effective Hamaker constant for separations greater than 50 nm tends towards the bulk value of mica and for separations less than 25 nm towards the value for stearic acid.

This completes our comparison of experimental results with theory: in general the agreement is very good. Before concluding the paper with a general discussion we include a short digression on the role of surface forces in adhesion and surface energy.

*Van der Waals forces, adhesion and surface energy*

The results already described show that the Hamaker constant for stearic acid monolayers is about 75 % of that of mica surfaces covered with their customary adsorbed monolayer of water. Nevertheless, if the surfaces are brought into molecular contact it is observed that the force required to separate the monolayers is far less than that required to separate two mica surfaces. Further if we integrate the van der Waals forces using the deduced Hamaker constant, we may calculate the work done to separate two surfaces from an initial separation of, say, 0.2 nm to infinity. This provides a measure of the surface energy of the material. For the monolayers this gives a value of about 30 mJ m$^{-2}$. This is a reasonable value. For the clean mica (covered only with an adsorbed water film) the value is 40 mJ m$^{-2}$. This is wrong. We know from direct measurements of the work of separation (Bailey & Kay 1967) that the correct value for the surface energy of mica in air is nearer 300 mJ m$^{-2}$. We must conclude that with mica, since the normal van der Waals behaviour is observed down to a separation of 2 nm, there must be strong short range forces which come into operation at separations appreciably *less than* 2 nm. These dominate the adhesion and surface energy. By contrast with the fatty acid monolayers only van der Waals attractive forces are involved down to atomic separations.

## 4. Discussion

In order to calculate theoretical values for the Hamaker constants $A$ and $B$ the dielectric behaviour of the interacting media must be known preferably over the whole spectral range but particularly in the absorption regions. As this information is rarely available interpolation procedures are often used in the computations. Alternatively, and as we have done here, one may adopt models which suitably represent the dielectric behaviour of the media. Thus for a dielectric which shows one strong absorption peak at a frequency $\omega_0$ we may express its dielectric constant as

$$\epsilon(\omega) = 1 + \frac{\text{const.}}{\omega_0^2 - \omega^2 + \mathrm{i}\Delta\omega \cdot \omega}, \tag{23}$$

so that

$$\epsilon(\mathrm{i}\xi) = 1 + \frac{\text{const.}}{\omega_0^2 + \xi^2 - \Delta\omega\xi}, \tag{24}$$

which is real, so that substitution into equation (5) allows for easy integration. Equations (20) and (22) are derivable in this way.

Were a dielectric with such a simple dispersion formula to exist its dispersion force would be very easy to calculate accurately, being non-retarded at separations $D$ below $\lambda_0/2\pi$ and retarded above. Many dielectrics do indeed exhibit this type of behaviour over certain frequency ranges, muscovite mica being a case in point having strong absorption in the u.v. around 100 nm. For this reason it is possible to make fairly accurate estimates of the force constants $A$ and $B$ solving equations (20) and (7) in terms of one characteristic absorption frequency and the refractive index.

Mica has also sharp absorption peaks in the i.r. at 10000 and 21000 nm (Vedder 1964) which also contribute to the dispersion force. This contribution, though small in the region where the forces were measured, is non-retarded for $D < 10000\,\text{nm}/2\pi$, and retarded for $D > 20000\,\text{nm}/2\pi$. Thus above 50 nm where we have found the dispersion forces of mica to be retarded the i.r. contribution is still non-retarded. As the distance of separation further increases we may therefore expect the i.r. contribution to assume predominance over the u.v. until eventually the dispersion force becomes once again non-retarded. This, however, ignores temperature effects which also assume importance at larger separations.

Finally, it should be remembered that the experimental results quoted here are for crossed cylinders of muscovite mica separated in air, and that in view of the above remarks it would be unwise to generalize them to other materials. This is particularly true of the transition region which is highly dependent on the absorption spectrum, on the intervening material (in this case – air), as well as on the geometry of the bodies. Nevertheless, the results show clearly that within certain limitations inherent in the theory the van der Waals dispersion forces of mica surfaces as observed are in good agreement with theory for both non-retarded and retarded forces. Further, they provide for the first time a direct and detailed experimental analysis of the transition between these two modes of interaction.

We thank Dr P. G. Fox for many helpful discussions and to the Ministry of Technology (now Procurement Executive, Ministry of Defence) for a research grant to one of us (J.N.I.).

## References

Bailey, A. I. & Kay, S. M. 1967 *Proc. R. Soc. Lond.* A **301**, 47–56.
Black, W., de Jongh, J. G. V., Overbeek, J. Th. G. & Sparnaay, M. J. 1960 *Trans. Faraday Soc.* **56**, 1597.
Casimir, H. B. G. & Polder, D. 1948 *Phys. Rev.* **73**, 360.
Derjaguin, B. V., Abrikossova, I. I. & Lifshitz, E. M. 1956 *Q. Revs.* **10**, 295.
Dzyaloshinskii, I. E., Lifshitz, E. M. & Pitaevskii, L. P. 1961 *Adv. Phys.* **10**, 165.
Hunklinger, S. 1969 *Proc. Conf. Physics of Adhesion, Karlsruhe*, p. 48.
Israelachvili, J. N. 1971 *Nature, Lond.* **229**, 85.
Kitchener, J. A. & Prosser, A. P. 1957 *Proc. R. Soc. Lond.* A **242**, 403.
Koch, E. E. & Skibowski, M. 1971 *Chem. Phys. Lett.* **9**, 429.
Krupp, H. 1967 *Adv. Coll. Int. Sci.* **1**, 111.

Langbein, D. 1969 *J. Adhesion* **1**, 237.
Langbein, D. 1971 *K. Phys. Chem. Solids* **32**, 1657.
Langbein, D. 1972 *J. Adhesion* **3**, 213.
London, F. 1930 *Z. Phys.* **63**, 245.
London, F. 1937 *Trans. Faraday Soc.* **33**, 8.
McLachlan, A. D. 1963*a* *Proc. R. Soc. Lond.* A **271**, 387.
McLachlan, A. D. 1963*b* *Proc. R. Soc. Lond.* A **274**, 80.
McLachlan, A. D. 1965 *Discuss. Faraday Soc.* **40**, 239.
Ninham, B. W. & Parsegian, V. A. 1970 *J. chem. Phys.* **52**, 4578.
Power, E. A., Meath, W. J. & Hirschfelder, J. O. 1966 *Phys. Rev. Lett.* **17**, 799.
Rouweler, G. C. J. & Overbeek, J. Th. G. 1971 *Trans. Faraday Soc.* **67**, 2117.
Schoen, R. I. 1962 *J. chem. Phys.* **37**, 2032.
Sparnaay, M. J. 1952 Thesis, Utrecht.
Sparnaay, M. J. 1958 *Physica* **24**, 751.
Sparnaay, M. J. & Jochems, P. W. J. 1960 *Third Int. Congr. on Surface Activity, Cologne*, 2, B/**111**/**1**, 375.
Tabor, D. & Winterton, R. H. S. 1969 *Proc. R. Soc. Lond.* A **312**, 435.
Van Kampen, N. G., Nijboer, B. R. A. & Schram, K. 1968 *Phys. Lett.* A **26**, 307.
Van Silfhout, A. 1966 *Proc. K. ned. Akad. Wet.* B **69**, 4, 501.
Vedder, W. 1964 *Am. Miner.* **48**, 736.
Winchell, A. N. 1954 *The optical properties of organic compounds*. New York: Academic Press.